Chapter 13
Insulated Autoclaved Cellular Concretes and Improvement of Their Mechanical and Hydrothermal Properties

Anna Stepien, Ryszard Dachowski, and Jerzy Z. Piotrowski

Abstract Materials forming the external building envelope, and in particular, thermal insulation are important factors in mitigating heat losses from a building, and thus reducing the overall building energy usage (i.e., lower energy consumption and costs of space conditioning energy). They also contribute to the improvement of building environmental characteristics through lowering the Greenhouse Gas (GHG) emissions and are now the object of a growing interest associated with sustainable construction trends. Autoclaved aerated concrete (AAC) and autoclaved cellular concrete (ACC) are widely considered as structural materials of improved thermal insulation characteristics. They are made with fine aggregates, cement (or cement and lime), and an expansion agent that causes the fresh mixture to rise like a bread dough to create a porous, thermally insulating concrete structure. In fact, this type of concrete contains about 80% of air, where one m^3 of raw materials is sufficient to produce around five m^3 of AAC. Depending on the bulk density and humidity, aerated concretes exhibit very unique thermal performance and hygrothermal characteristics. This fact is of particular importance when designing building envelopes of optimized R-value (thermal resistance), or U-value (heat transfer coefficient). Typically, the thermal conductivities of AAC and ACC are a function of material density and moisture content that range from 0.1 to 0.7 W/(m·K) for material densities between 400 and 1700 kg/m^3. This chapter discusses the physical properties of cellular concretes. Efforts to improve the mechanical and insulation performance characteristics using high-performance polystyrene (HIPS) are discussed. To analyze the geometry, size, and distribution of concrete pores in AAC with added HIPS, a series of measurements were performed by the authors. This includes analysis of concrete density, as well as porosity testing and Micro CT analysis (CT—computerized tomography). These tests show the presence of one nm pores, and the volume

A. Stepien (✉) · R. Dachowski
Faculty of Civil Engineering and Architecture, Kielce University of Technology, al. 1000-lecia PP 7, 25-314 Kielce, Poland
e-mail: Ana_stepien@wp.pl; a.stepien@tu.kielce.pl

J. Z. Piotrowski
Faculty of Environmental, Geomatic and Energy Engineering, Kielce University of Technology, al. 1000-lecia PP 7, 25-314 Kielce, Poland

J. Kośny and D. W. Yarbrough (eds.), *Thermal Insulation and Radiation Control Technologies for Buildings*, Green Energy and Technology,
https://doi.org/10.1007/978-3-030-98693-3_13

of voids in the material was estimated at approximately 50%. In addition, to better understand the internal structure of the AAC material, the following analyzes were performed: XRF, XRD and SEM with the EDS analyzer (Energy Dispersive X-ray Spectroscopy).

Keywords Autoclaved aerated concrete (AAC) · Thermal isolation · Micro CT · Pores · Microstructure · Autoclaved cellular concrete (ACC)

13.1 Introduction

The climate change, which was partly caused by extensive activities in the construction sector, is still progressing with constant intensification. That is why today, energy efficiency has become the mandatory point of interest during the design of modern, sustainable, and durable buildings. Sustainable building design practice and a usage of natural resources, combined with effective operation of mechanical systems and whole facilities, are essential for construction of so-called green, low-energy buildings—see: Birkenmajer (1967), Kozłowski (1975), Parker and Lilly (2005), Skalmowski (1966). They are also expected to reduce the occurrence of construction failures and extend overall building lifespan.[1]

In 2008, European Union countries introduced energy performance certificates for buildings (Directive 2002/91/EC of 16 December 2002[2]) for new and renovated buildings. All these steps are expected to contribute to beneficial environmental changes and optimization of manufacturing and construction processes—see: Boltyanskii et al. (1995), Polyzois and Raftoyiannis Ioannis (2007), EU PN (2004). Building envelope materials, structural components, and construction methods play a very important role in this initiative. Lightweight aerated concretes can simultaneously serve as a thermal insulation and a structural support material. A building envelope should be designed to control the flow of air, heat, sunlight, radiant energy, liquid water, and water vapor. It should also provide many other attributes including fire protection, noise control, impact damage resistance, durability, aesthetic quality, and affordability—Szoke (2014).

Aerated concretes are materials that are characterized by low density, good thermal insulation characteristics and mechanical strength. They are non-flammable and are considered as natural due to their material composition. Autoclaved aerated concretes (AAC) or autoclaved cellular concretes (ACC) are made with fine aggregates, cement (or cement and/or lime), and an expansion agent that causes the fresh concrete mix to rise like a bread dough. In fact, this type of concrete may contain in its pores over 80% air. In concrete plants where AAC is made, the material is molded, expanded, and cut into blocks, panels, or beams (Figs. 13.1 and 13.3). During construction, AAC or ACC blocks or panels are usually joined together with a thin bead mortar. AAC or ACC components can be used for construction of walls, floors, and roofs. These

[1] https://cembureau.eu/library/reports/2050-carbon-neutrality-roadmap.

[2] https://eur-lex.europa.eu/legal-content/EN/TXT/?uri=celex%3A32002L0091.

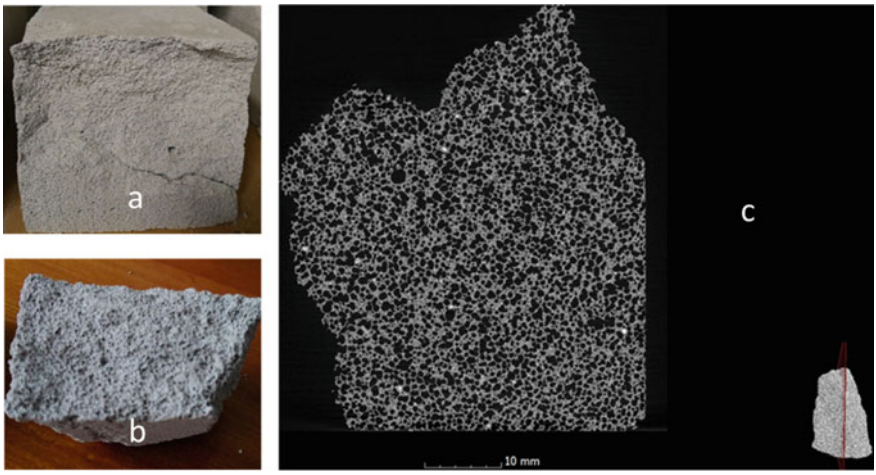

Fig. 13.1 Autoclaved aerated concrete—**a** laboratory sample, **b** texture of AAC after the break, **c** relatively uniform micro-porous structure of AAC, visible in micro-CT analysis

lightweight construction materials offer excellent sound and thermal insulation, and like all cement-based materials, are mechanically strong and fire resistant.[3]

AAC is made mostly of natural materials such as quartz sand, water, lime, cement, i.e. with possible replacement of significant portions of cement by fly ash or other natural pozzolans. AACs are often considered as sustainable, or environmentally friendly. Furthermore, some researchers and AAC producers claim that manufacturing procedure requires lower energy input than the production of other construction materials or their components—Brelak and Dachowski (2017a).

The important early developments in the field of aerated concretes took place at the end of the nineteenth century. In 1880, a German researcher Michaelis was granted a patent on his concrete steam curing processes. A little bit later, Hoffman, a Czech, successfully tested and patented in 1889 the method of "aerating" concrete by carbon dioxide. Probably, the most meaningful event in history of cellular concrete, however, was the development of a method of scarifying cellular concrete using aluminum powder. This technology was patented in 1914 by two Americans, Aylsworth and Dyer. They used aluminum powder and calcium hydroxide to attain a porous cementitious mixture. This method is still used by almost all cellular concrete manufacturers, despite many years of research in this field. Following this development, in Europe, Axel Eriksson, a Swede, made several serious follow-on steps towards developing a modern AAC. In 1920, he patented the method of making an aerated mix of limestone and ground slate (a so-called "lime formula"). Next, in 1923, he invented the most advantageous way of curing cellular concrete in autoclaves using hot steam.

[3] https://www.cement.org/cement-concrete/paving/buildings-structures/concrete-homes/building-systems-for-every-need/autoclaved-aerated-concrete.

The emergence of autoclaved cellular concrete technology can be attributed to the energy crisis, which occurred in the 1930s in Sweden, when drastic restrictions were placed on the use of wood for building purposes. This was the first step towards the use of AAC, a material that combines some benefits of wood, such as good thermal insulation, natural origin of raw materials, lightness and ease of processing and construction, while being free of many wood disadvantages, i.e. AAC is resistive to decaying and it is non-flammable—see: Lothenbach et al. (2019), Błaszczyński and Król (2014). Due to its porous structure, cellular concrete is also a material with higher thermal insulation properties when compared to other types of concretes. It is also suitable for a usage as a load-bearing material, because it exhibits compressive strength in the range of 2–6 MPa.[4] Today, AAC masonry blocks are considered in many parts of the world as a prime construction material for residential and small commercial buildings. They are widely used in single-family homes as well as in other types of up to three-story commercial buildings, or other load-bearing structural applications. In addition, AAC, due to its ability to efficiently regulate the indoor air humidity, is widely regarded as a healthy material, showing a positive impact on the well-being of building residents. It is capable of absorbing the excess moisture from the room and return it back when the air becomes too dry. In addition, AAC exhibits a valuable resistance to bacteria, molds, and fungi. This is due to its chemical composition and resulting strong alkaline pH, which doesn't promote the growth of microorganisms.[2]

During the past century (mostly after WWII), the production technology of AAC products has been constantly improved. Today, specially designed, autoclave facilities are used worldwide to produce AAC building products. With small custom differences, AAC production procedures are similar in most production facilities worldwide. At the beginning of the production process, the lime is pre-homogenized with complete internal reaction for a period of time after ground.?????? According to the example given by Li et al. (2020), the aluminum paste is dissolved in water at room temperature. It is later added to other components to create a concrete slurry, which is made at temperature of ~40 °C. During the next processing step, the slurry is cast into a mold preheated to a temperature of around 50 °C, where it later stays for about 30 min at a temperature of 64 °C, to complete the process of foaming, thickening, and hardening. After demolding, the blocks are placed into the autoclave for steam-curing for about three hours at pressure of 1.0 MPa and ~~the~~ temperature of 185 °C—Li et al. (2020).

Due to the growing awareness of environment problems, and the global sand supply deficit, many traditionally used AAC raw materials are being replaced now by various industrial by-products, and waste products (including waste concrete). That is why today, AAC products may embrace a waste containing mainly silicon and calcium, as well as other industrial by-products such as: fly ash, silica dust, bottom ash, waste from iron ore processing, copper waste, and slag blast furnace. It has been well researched and documented that a partial replacement of cement by the fly ash and/or other natural pozzolans significantly lowing the Global Warming Potential

[4] https://www.solbet.pl/en/technical-parameters.

(GWP) of concrete products—Wcisło (2018). Crushed waste concrete aggregates (fine) and concrete powder are sometimes used as a replacement of natural sand and fine aggregates in AAC.[3] In addition, studies show also that the use of rice husk ash can be utilized as a partial replacement for fine aggregate reduces the strength and density of AAC with a tendency to shorten the autoclaving time and the required autoclaving temperature.[5] Efforts have been made to improve the mechanical properties, especially fracture toughness, and increase the thermal insulation performance of AAC by using wood fiber and rubber powder—Szoke (2014). It was shown that the thermal conductivity of AAC with this modification increased linearly and was dependent on the basalt fiber content (the greater the amount of basalt fiber, the higher the strength parameters for the tested material). The strength parameters of AAC are closely related to its internal porous structure. Therefore, regardless of the substrates and modifiers used, AAC products are usually good thermal insulators, which exhibit sufficient strength (for non-load-bearing structures) and durability.

According to the American Concrete Institute (ACI)—ACI-122R-14 "Guide to Thermal Properties of Concrete and Masonry Systems" (Szoke (2014)) thermal conductivity of the AAC blocks ranges between 0.1 and 0.7 W/(m·K) for a density of 400–1700 kg/m^3 The impact of moisture on the steady-state and dynamic thermal performance of AAC walls in residential and commercial buildings located in California, U.S. were analyzed by Gawin and Kośny (2000), Gawin et al. (2004). Thermal conductivities of five types of AAC and several lightweight walls, were measured in laboratory conditions, at various moisture contents. Then, the moisture distribution in AAC walls was simulated for California climate using the coupled heat and moisture transfer numerical model. Hygrothermal simulations were followed with whole building energy modeling for a single-story residential home. The whole building energy simulation results indicated a superior performance of AAC walls, compared to other types of lightweight systems of identical thermal resistance.

The following North American building standards regulate material characteristics and assembly methos for AAC masonry products:

- ASTM C1691-11 (2017) Standard Specification for Unreinforced Autoclaved Aerated Concrete (AAC) Masonry Units.[6]
- ASTM C1693-11 (2017) Standard Specification for Autoclaved Aerated Concrete (AAC).[7]

In Europe, the product standards for masonry units—including those for AAC units—have been under new regulation since April 1, 2006. Following the end of the coexistence period for the national and European standards, the harmonized European product standard DIN EN 771-4 was implemented. On November 1, 2015, Part 4 in the specification for masonry units was introduced: Autoclaved aerated

[5] https://www.irjet.net/archives/V7/i2/IRJET-V7I2279.pdf.

[6] https://www.astm.org/Standards/C1691.htm.

[7] https://www.astm.org/Standards/C1693.htm.

concrete masonry units (includes Amendment A1:2015). This standard specifies the characteristics and performance requirements of AAC masonry units.[8]

Similarly, in China, the thermal conductivity of AAC blocks used in civil construction ranges from 0.13 to 0.22 W/(m·K) for concrete density in the range 400–700 kg/m^3. The national standard GB/T 11,969-2008, "Test Methods of Autoclaved Aerated Concrete" describes test methods for AAC masonry products.[9] According to Chinese building standards, the thickness of external walls built of AAC blocks should be no less than 400 mm and 300 mm, for residential buildings in a very cold climatic zone and a cold zone, respectively[3]—Li et al. (2020).

13.2 Fabrication of Autoclaved Aerated Concrete (AAC) and Description of the Autoclaving Process

There are two groups of concrete products manufactured by autoclaving: autoclaved aerated concrete (AAC) and lime-sand products commonly known as silicate bricks. In both cases, sand and water are basic raw materials used in their production. For aerated concrete, cement is also added. There is also a second category of lightweight cellular materials produced industrially. This second variant of lightweight cellular concrete is a foamed concrete, which it usually produced in field conditions. This technology, however, has not yet been used on a wide scale—Dachowski and Kapała (2016).

Aerated concretes are materials that are characterized by low density, good thermal insulation, flame resistance, and unique mechanical strength parameters. Masonry blocks that are made of ACC are usually about one-third of weight of similar products made from regular concrete. In addition, AAC products are flame resistance and do not contain any toxic gases or other toxic substances. They offer many advantages over traditional wood construction, while being free of many wood disadvantages. For example, AAC is dimensionally stable with no deflections or warping caused by changing moisture conditions. This improves the overall product durability—see: Lothenbach et al. (2019), Błaszczyński and Król (2014). AAC panels and blocks are produced in factories to exact specified sizes. There is almost no need for on-site trimming since blocks and panels fit so well together, there is also little need for use of finish materials such as mortar. If needed, AAC products can be easily cut with hand tools on the construction site. Finally, because of low thermal conductivity, 24–36 cm thick walls, made of AAC blocks, can easily fulfill, building code requirements in many severe climates worldwide, without a need for additional sheathing thermal insulation—see: Lothenbach et al. (2019), Błaszczyński and Król (2013), Zapotoczna-Sytek (2018). The major disadvantages of cellular concrete blocks include: high water absorption, and relatively low compressive strength, compared to other concrete products (up to 6 MPa on average). From the structural

[8] https://standards.globalspec.com/std/9975426/DIN%20EN%20771-4.

[9] https://www.doc88.com/p-3854253232623.html.

perspective, AAC is a material of mechanical strength allowing the construction of load-bearing structural walls in buildings for up to 3–4 floors (depends on the local country building standard regulations, specific for different product types). There is also a group of reinforced AAC technologies, allowing fabrication of a variety of structural building elements such as ceiling beams, columns, headers, and roof rafters.

The small-scale production of AAC masonry products started in Sweden in the 1930s. However, the real beginning of a widespread cellular concrete production on the industrial scale in Europe dates back to the 1940s and continued until the 1970s. Later, during the 1980s, numerous AAC plants built in Asia, the Middle East and Eastern Europe were based on four major technologies developed in Europe by Siporex and Ytong (Sweden), Durox (Netherlands), and Hebel (Germany). In the beginning of the 1990s, the first AAC production plant based on the Ytong technology was supplied to China. In Poland, this development is associated with a patented production method referred to as "the universal Polish method" called Unipol.[10] In spite of the fact that the AAC fabrication technology is similar worldwide (with several proprietary variations), depending on the manufacturer and the intended use, cellular concrete masonry and panel products are made in slightly different ways. In these processes, Portland cement, burnt lime, and some aggregates are used to prepare a binder, all together ground dry. When the fly ash (most often sourced from coal combustion) is utilized as the cement substitute, gypsum dihydrate (gypsum rock) is added as a dry additive. Quartz sand and/or fly ash are often used as aggregates. Water is the third, main component of the cellular concrete mix. It is added in the amount of 0.9 l/m^3 of semi-liquid concrete mix. A skimmed, flakey aluminum powder or aluminum paste is used for the foaming step (aeration). During the AAC production, gypsum can be also added to act as a setting regulator[9]—Zapotoczna-Sytek (2018).

Today, AAC manufacturing is carried out according to strictly followed material recipes and operation processes. The most important preparatory tasks include: (i) preparation of raw materials (this often includes drying, grinding, or heating materials, or mixing with water), (ii) dosing the ingredients in accordance with the specific company recipes, and (iii) mixing the whole batch. Examples of typical concrete formulations, used by major European AAC companies are presented in Table 13.1—Brelak and Dachowski (2017a).

Following the material mixing, the aerating agent reacts with the calcium hydroxide and causes the release of hydrogen, which escapes from the mix, causing it to rise, and creating thousands of small cells with air trapped in them. Today, cellular concretes of various bulk densities are produced following proprietary company-specific formulations and fabrication methods. The target AAC porosity is between 60 and 85%. That is why, the solids surrounding the pores shouldn't account for more than 40% of the total volume of used materials. At the end of this part of production, (v) an additional waiting period is needed for the concrete mix to harden, and later (vi) for slicing the hardened mass into pieces of appropriate dimensions. The surplus

[10] http://www.eastlandchina.com/60-years-of-aerated-concrete-in-Poland-The-Past-and-the-future-id37144.html.

Table 13.1 Typical concrete mix formulations used by European AAC companies

Company	Basic substrates		Method of preparing ingredients
	Binder	Aggregates	
YTONG	Quicklime + cement (or blast furnace slag)	Quartz sand and, bottom ash	Dry milling of binder and aggregate or milling of aggregate with water and lime
SIPOREX	Cement	Sand or sand with blast furnace slag	Grinding sand and slag with water into sludge
HEBEL	Cement + quicklime	Quartz sand	Grinding sand with water into sand sludge
Calsilox	Cement + quicklime	Quartz sand	Common dry milling of binder and aggregates

Source Brelak and Dachowski (2017a)

concrete mix left over after the processing is returned to the component mixer, so the production is almost waste-free and consequently doesn't impact the environment through waste generation. The next production stage involves (vii) bringing the pallets with the hardened products to the autoclave, where the concrete is finally set. For this purpose, saturated autoclavation is associated with a process of curing the concrete mix in hermetically sealed autoclaves which are auxiliary heated for up to 12 h. Thanks to autoclaving, the chemical shrinkage of material is minimized. This improves the AAC frost resistance, increases durability and mechanical strength. At the final stage, hardened AAC products are subjected to a quality check and then stored in controlled environmental conditions—see: Stepien et al. (2019), Wcisło (2018), Lothenbach et al. (2019).

In autoclaves, under conditions referred to as hydrothermal, chemical reactions take place that guarantee the strength and quality of resulting products. As mentioned earlier, the combination of cement, lime, gypsum (anhydrite), finely ground sand and most importantly aluminum powder or paste causes the whole mix to considerably expand. During this process, the following three-step chemical reaction takes place (in simplified form):

1. $CaO + H_2O \rightarrow Ca(OH)_2 + 65{,}2$ kJ/mol
2. $3Ca(OH)_2 + 2Al + 6H_2O \rightarrow Ca_3(Al(OH)_6)_2 + 3H_2$
3. $6SiO_2 + 5Ca(OH)_2 \rightarrow 5CaO\ 6SiO_2\ 5H_2O$.

The final product of this process is Tobermorite or Hydrated Calcium Silicate $C_5Si_6H_5$—see: Van Boggelen (2014).

During AAC production the temperature in autoclaves depends on the pressure used. The increase of the autoclave pressure allows a usage of higher processing temperatures—Lothenbach et al. (2019).

As a part of ecological construction trends in cement and concrete industries, a new material solution, utilizing a geopolymeric cement binder has been introduced.[11] This alkaline-activated binder is not based on calcium carbonate chemistry—see: Matschei et al. (2007). It generates significantly lower CO_2 emissions and exhibits better strength than classic clinker-based cement. The procedure for production of geopolymer-based light-weight material similar to AAC blocks was recently developed—Kejkar Rupali and Wanjari Swapnil (2021). In this case, chemically aerated geopolymer material, resembling a foamed concrete was developed at a high alkaline solution concentration.

When compared to the conventional AAC manufacturing, this novel processing involves higher temperature, sometimes requires increased duration of the heat curing process, and higher pressure, which pose challenges for commercialization. In a recent study that focused on manufacturing of geopolymer-based aerated concrete, granulated blast furnace slag was utilized as an alternate to cement content (with 10–30% load). This new geopolymer-based foamed material is heat cured at 100 °C for a three-hour time period. The final product demonstrated 4.8 MPa compressive strength and contained 60% of fly ash, 30% of granulated blast furnace slag, and only 10% of Portland cement— Kejkar Rupali and Wanjari Swapnil (2021).

13.3 Basic Technical Characteristics of AAC

13.3.1 Density and Compressive Strength

Cellular concretes (Fig. 13.1a, b), depends on their average dry bulk density, are usually divided into the following concrete classes: 400, 500, 600 and 700 (Table 13.2). For these varieties, the lower and upper limits of volumetric density and corresponding product labels, i.e., the average values of compressive strength in the dry state, have been determined by AAC manufacturers. A comparison of the bulk density of cellular concrete with regular concrete products shows that it is 1/3–1/2 the density of regular concretes and has significantly lower thermal conductivity than regular concrete.

Autoclaved cellular concrete can therefore be used to manufacture large, lightweight products which can be combined with conventional masonry or other building envelope materials. The compressive strength of cellular concrete depends on its bulk density, and it is between 2 and 6 MPa (as discussed in Stepien et al. (2019), Nonat and Lecoq (1998)), while tensile strength represents 20–40% of compressive strength, similarly, shear strength is 20–30% of compressive strength. The modulus of elasticity is in the range 1.5 and 2.6 MPa. The water content of a specimen during testing and the direction of crushing in relation to the direction of the concrete growth in the mold are also important. In European standards, the compressive strength is

[11] https://www.nbmcw.com/product-technology/construction-chemicals-waterproofing/concrete-admixtures/geopolymer-concrete-the-eco-friendly-alternate-to-concrete.html.

Table 13.2 Approximate amounts of components in the production of AAC by the Unipol method, for 500, 600 and 700 concrete classes (density classification)

Composition of the mixture	Unit	Sand technology			Ash technology		
		260	600	700	500	600	700
Sand	dcm^3	260	350	440	–	–	–
Fly ash	kg	–	–	–	270	360	450
Binder	kg	240	260	280	230	240	255
Water	dcm^3	80	75	62	250	300	350
Aluminum powder	kg	0.47	0.41	–	0.44	0,35	0.30
Surface active agent	dcm^3	1.5	1.5	1.5	1.5	1.0	1.0

Source Lothenbach et al. (2019), Błaszczyński and Król (2014), Zapotoczna-Sytek (2018)

determined at a stabilized water content of approx. 6 wt.%. This is 80% of the compressive strength in the dry state, determined according to PN-89/B-06258,[12] EN 771-4,[13] and EN 772-16.[14]

13.3.2 Thermal Conductivity

The thermal conductivity of cellular concretes depends on their density and the water content. Several companies are currently able to produce AAC products with densities in the range 300–800 kg/m^3, with lambda values as low as 0,08 W/(m·K)—Pruteanu and Vasilache (2013). Additionally, the required compliance with the strict EU standards (EN 771-4 and EN 772-16) results in high-precision products (tolerances of <1 mm for blocks and <3 mm for panels). This allows utilization of AAC products, which is associated with the on-site use of a thin bed mortar instead of a thick layer of conventional mortars. This reduces thermal bridging (improving thermal performance) and decreases the total cost of construction. Furthermore, the production of ultra-lightweight AAC blocks with thermal conductivity as low as 0,045 W/(m·K), at density of 145 kg/m^3, has already become possible for some AAC producers—Van Boggelen (2014).

[12] https://www.iso.org/standard/66185.html.

[13] https://infostore.saiglobal.com/en-us/Standards/EN-771-4-2011-A1-2015-331270_SAIG_CEN_CEN_761852/.

[14] https://www.en-standard.eu/bs-en-772-16-2011-methods-of-test-for-masonry-units-determination-of-dimensions/.

13.3.3 Frost Resistance

The water absorption of cellular concrete is between 40 and 60 vol.%, i.e. approx. 25% lower than would result from its total porosity. This means that the cells do not fill up completely when water is absorbed. This fact has a positive effect on frost resistance. The freezing water in the cell increases volume by about 10%. However, due to available extra cell volume, this does not exert pressure on the cell walls and thus does not induce undesirable stresses on the concrete structure.

13.3.4 Fire Resistance

Fire resistance is one of the most important building code requirements for construction products. The fire resistance is the ability of a structure element to withstand the action of fire under certain mechanical effects on one or more surfaces for a specified period of time without losing its load-bearing properties (PN-EN 13,501-2). Construction products manufactured and sold in the territory of the European Union are classified according to the PN-EN 13,501-1 standard, which provides for seven basic classes: A1, A2, B, C, D, E, F[15]—Macech (2020). Masonry walls made of cellular concrete blocks in the thickness range of 180–360 mm meet the requirements for the highest class of fire resistance of buildings as they withstand a 240 min fire test[15],[16]—see: Dachowski and Kapała (2016), Kapała and Dachowski (2016), Brelak and Dachowski (2017a), Macech (2020).

13.3.5 Natural Radioactivity

Building occupants are continuously exposed to radiation emitted by building materials. Construction materials produced from natural mineral sources such as rocks and/or soil, usually contain small amounts of natural radionuclides of the uranium (^{238}U), thorium (^{232}Th) series, and potassium (^{40}K). These radionuclides can cause external and internal radiation exposure to occupants. While, the external exposure is usually caused by direct gamma radiation, the internal radiation exposure, often affecting the respiratory tracts, is due to radon and radon decay products, which radiate off from building materials. Good knowledge of the basic radiological characteristics such as radioactive content in building materials is important in the assessment of possible radiation exposure to the population. It is also essential for the development of building standards and material usage guidelines. In Poland,

[15] https://www.en-standard.eu/bs-en-13501-1-2018-fire-classification-of-construction-products-and-building-elements-classification-using-data-from-reaction-to-fire-tests/.

[16] https://www.itb.pl/badania-ogniowe.html.

Table 13.3 The content of natural radioactive isotopes—Kapała and Dachowski (2016)

Building/construction material	$f_1 < 1.2$*	$f_2 < 240$ Bg/kg** (radioactive activity***)
Sand-lime brick	0.16	20
Aerated Autoclaved Concrete made with sand	0.16	20
Concrete	0.22	24
Expanded clay aggregate	0.36	32
Ceramic brick	0.54	70
Breezeblock (slag/cinder) block	0.56	80
Cellular ash concrete	0.60	90

* Dimensionless coefficient f1 is expressing the content of natural isotopes of ^{40}K, ^{226}Ra, ^{228}Th
** Content of ^{226}Ra expressed in Bq/kg
*** Radioactive activity is a physical quantity equal to the rate of radioactive decay of atomic nuclei of a given sample, expressed in becquerel, Bq: 1 Bq = 1 decay/1 s. [see: Piotr Jaracz: Promieniowanie jonizujące w środowisku człowieka. Fizyka, skutki radiologiczne, społeczeństwo. Ionizing radiation in the human environment. Physics, Radiological Effects, Society. Warsaw, Poland: Wydawnictwa Uniwersytetu Warszawskiego, 2001. ISBN 83-235-0146-7]

a systematic study of natural radioactivity of building products, including cellular concrete, has been carried out since 1980 (see: Table 13.3).

13.4 Enhancement of Mechanical Strength Characteristics of AAC by Use of High Impact Polystyrene (HIPS-High Impact Polystyrene)

When compared to regular density concretes, aerated concrete is characterized by relatively low compressive strength, typically ranging from 2 to 6 MPa. One of the methods of improving the compressive strength is the modification of aerated concrete with high-impact polystyrene (HIPS). HIPS is a thermoplastic polymer obtained by the block-suspension polymerization of styrene with an addition of synthetic rubber. As a result of polymerization, small particles of polybutadiene remain in the polystyrene matrix, changing its physical and mechanical properties[17]—see: Abdulrahman and Bruce (2004), Vilaplana et al. (2010), Alfarraj and Nauman (2004). HIPS thus achieves better temperature stability and plastic stiffness, which helps improve performance of building materials (e.g. concrete) modified by the addition of HIPS. Cellular concretes are not resistant to mechanical damage. That is why HIPS is used in AAC to increase the hardness of the material while maintaining its thermal performance. A recent study showed that the modification of AAC

[17] http://www.plastics.pl/produkty/tworzywa-techniczne/polistyren-ps/polistyren-wysoko-udarowy-hips.

Table 13.4 Tests which were performed on AAC specimens enhanced with HIPS

Research	Characteristics of the study
Calorimetry	Measurement of heat generated by chemical reactions and various physical processes
Porosimetry	Pore size and distribution analysis using Mercury Porosimeter SYL & ANT Instruments, Micrometrics (AutoPore IV)
SEM—scanning electron microscope	Microscopic analysis to visualize the microstructure of the modified material. Microstructural characterization and elemental analysis of the samples were performed using Scanning Electron Microscopes (Quanta FEG 250 FEI)
X-ray diffraction (XRD)	XRD is a non-destructive test method used to analyze the structure of crystalline materials. XRD measurements of powdered samples were conducted with Empyrean PANalytical diffractometer using Ka radiation from a Cu anode
X-ray fluorescence	Elemental composition testing using the PANalytical instrument (XRF)
Micro CT analysis	Industrial computed tomography—non-surface analysis and visualization studies providing insight into the inside of the material (microscope Nikon XT H 225 ST—see: Fig. 13.1c)

with HIPS increased the compressive strength of the material by 27% and decreased the water absorption factor by 28% in comparison to a conventional product—see: Nonat and Lecoq (1998), Stepien et al. (2020). The material used in the tests was a re-granulate, pulverized to 630 μm particle size, with a density of 1.05 g/cm^3. A series of tests was performed on HIPS-modified AAC cube specimens (100 mm edge length), made under semi-industrial conditions in the aerated concrete manufacturing plant following a slow-setting silicate technology (SW) as a 500 concrete variant (gross dry density class).[18] The SW technology involves producing a slurry from adequately proportioned components (sand and gypsum jointly account for about 72% of the product mass, cement, and lime—about 20% and water—about 7%). At this stage, appropriate quantities of the HIPS were added. After mixing, the slurry was placed in tripart molds and stored in curing chambers at 60 °C for three hours. After that, the specimens were placed in autoclaves for 13 h at a temperature of 190 °C and a steam pressure of 1.2 MPa—see: Zapotoczna-Sytek and Balkovic (2013), Abdulrahman and Bruce (2004), Rybarczyk et al. (2015). Figure 13.3 shows samples of analyzed AAC material. Table 13.4 lists the tests which were performed to analyze the structure and properties of the AAC enhanced with HIPS:

[18] https://www.solbet.pl/zalety-betonu-komorkowego/gestosc-betonu-komorkowego/.

Table 13.5 XRF analysis of AAC with HIPS

Formula	Concentration (%)
CaO	50.377
SiO_2	39.280
Fe_2O_3	3.534
SO_3	2.859
Al_2O_3	1.908
MgO	0.313
K_2O	0.813
SrO	0.111
TiO_2	0.527
P_2O_5	0.113
MnO	0.064
ZrO_2	0.052
ZnO	0.049

The above tests were performed based on the CEN standards: PN-89/B-32250,[19] PN-EN 1008:2004[20] and based on the available construction regulations.

As presented in Table 13.5, the XRD analysis of elemental composition showed the main components of AAC are: SiO_2, CaO, Fe_2O_3, Al_2O_3, SO_3, MgO, K_2O. The distribution and arrangement of pores that are present in the specimen of AAC that was tested using optical microscope, as well as XRD and micro-CT analyses.

AAC is a material that undergoes binder hydration. The next test that was performed was calorimetry.[21] The hydration process takes place immediately after the binder (cement, lime) is combined with water in the presence of other components of the raw mass (quartz sand, additives). However, hydration can also occur over time under certain hydrothermal conditions.

The thermal effect of many transformations is difficult to measure because it may be accompanied by other side processes, which themselves absorb or produce thermal energy—Van Boggelen (2014). A process of forming/setting of the AAC's internal microstructure is very dynamic and it is extremely important to understand the thermodynamic behavior of its components and phases that are formed. In ACC, hydrated calcium silicates are present, which are stable in certain temperature ranges and the stability of these products also depend on this factor (Calcium-Silicate-Hydrate phase or Tobermorite, although it is not always desirable in concretes, including ACC). Isothermal titration calorimetry (ITC) is a technique used to quantitatively study interactions between molecules. It directly measures the heat that is released or

[19] https://sklep.pkn.pl/pn-b-32250-1988p.html.

[20] https://sklep.pkn.pl/pn-en-1008-2004p.html.

[21] https://apinstruments.pl/izotermiczna-kalorymetria-miareczkowa-itc/.

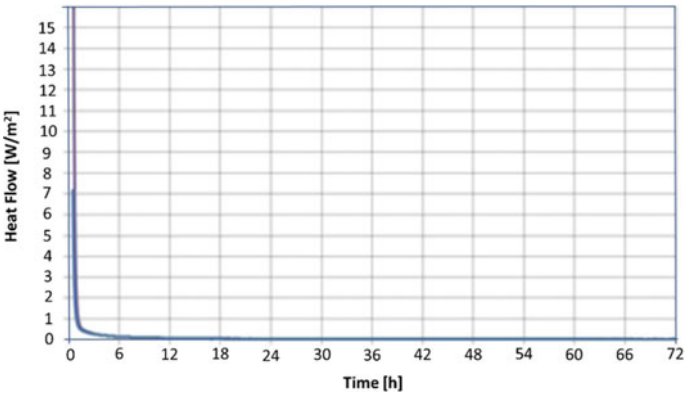

Fig. 13.2 Heat flow recorded during the hydration process in AAC samples containing HIPS—measured using isothermal titration calorimetry (ITC)

absorbed during bond formation. ITC is the only method that simultaneously determines all binding parameters in a single experiment and does not require any modification of the reactants involved in the binding. Measurement of heat flow during binding enables accurate determination of the binding constant (KD), reaction stoichiometry (n), enthalpy change (ΔH) and entropy change (ΔS), which contributes to a complete thermodynamic profile of the interaction between molecules—see: Rybarczyk et al. (2015). The test data presented in Fig. 13.2 indicates that hydration occurred only during the first phase of the ACC setting process and any subsequent changes were not observed.

13.4.1 Mechanical Strength Properties and Porosity of ACC Modified with HIPS

In earlier studies, strength and water absorption measurements were used for conventional AAC and similar cellular concrete modified with HIPS (AAC with HIPS). Basic properties of both analyzed materials are presented in Table 13.6. The high-impact plastic used for AAC enhancement is a waste product that, as a result of this modification, positively improved the physical and mechanical properties of

Table 13.6 Compression strength and water absorption for analyzed aerated concrete products

Materials (AAC)	Average compressive strength (MPa)	Average water absorption coefficient ($g/m^2 * s^{0,5}$)
AAC	3,35	105
AAC with HIPS	4,70	66

Source Dachowski and Kapała (2016)

the tested product. As shown in Table 13.6, the addition of HIPS to AAC yielded about a 40% increase in compressive strength and decreased the coefficient of water absorption of about 37% when comparing to conventional AAC without HIPS—see: Dachowski and Kapała (2016).

As shown in Fig. 13.3a, density tests were performed using the Quantachrome Ultrapyc 1200e helium pycnometer. Irregularly shaped concrete specimens of 10–25 g were used for this purpose. For the porosimeter tests, the specimens were sequentially placed in the low-pressure port, where they were evacuated to 2.66 Pa and flooded with mercury at 0.035 MPa.—see: Fig. 13.3b.

Figures 13.4, 13.5, 13.6, 13.7 and 13.8, show the distribution and size of pores in the specimens R1, R2, R3, and R4. R1 is the reference AAC material while R2, R3, R4 is a modified HIPS material in the amount of 10, 20, 30%. In AAC production, it is not recommended to use a larger amount of the additive due to the possibility of cracking of the starting material (HIPS, like some mortars, may show high strength, which may result in cracking during operation). The tests showed that the specimens with HIPS addition showed a larger pore volume in the range (0.001–100), while the pore distribution was similar as in the reference material.

When analyzing the porosimetry results, it is important to remember that mercury is forced into pores of ~0.01 μm in diameter and smaller at very high pressures—over 100 MPa. Therefore, if the pores are connected by narrow passages and the specimen material cannot withstand this loading, the pores are sometimes crushed before mercury can penetrate. However, the possibility of injecting mercury into the bottle-neck pores without particularly destroying the material structure must not be overlooked. Otherwise, the theoretical calculation results may reflect the actual porosity values. Simply, the pore size distribution calculated from the MIP data will be inaccurate. In the case of large pores, with diameters around one μm, mercury is injected into them at a pressure of one MPa. A maximum pressure of 420 MPa

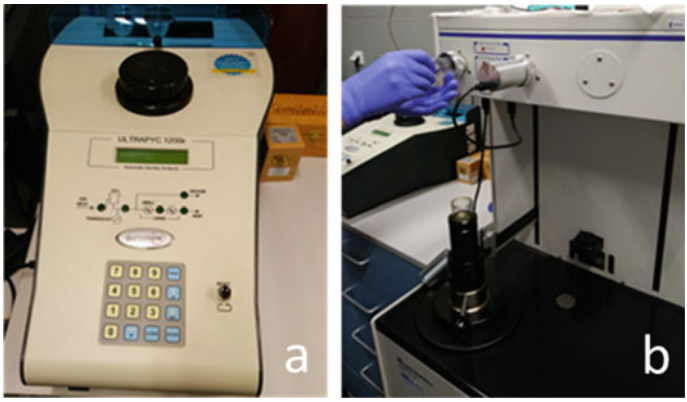

Fig. 13.3 Analysis of AAC pore sizes performed with a use of **a** helium pycnometer (QUANTACHROME ULTRAPYC 1200e) and **b** mercury porosimeter SYL & ANT instruments

is needed to force the mercury into pores with diameters of 0.006 μm. High pressures can destroy the internal skeleton and open access to pores that were completely isolated under natural conditions. If the assumption is made that the critical destructive pressure is close to the tensile strength of the material, when mercury is injected into pores with radius dimensions of ≤0.02 μm, an intense damage process that changes the picture of the actual pore distribution will begin.

The present discussion of the results of mercury porosimetry measurements is usually interpreted in terms of long cylindrical capillary bundles. Tests (density and porosimetry—Figs. 13.4, 13.5 and 13.6) were performed on 4 independent samples of ACC with HIPS. The sample R1 was used for the pore size analysis (Figs. 13.7 and 13.8). The plots of the cumulative pore volume against its radius were developed using the results from four tests performed on specimens R1, R2, R3, R4, (Figs. 13.5 and 13.6). It can be observed on Fig. 13.7. that the pore size of 10–50 μm has the largest volume in the sample, followed by 0.0025–0.004 and 0.01–0.04 μm.

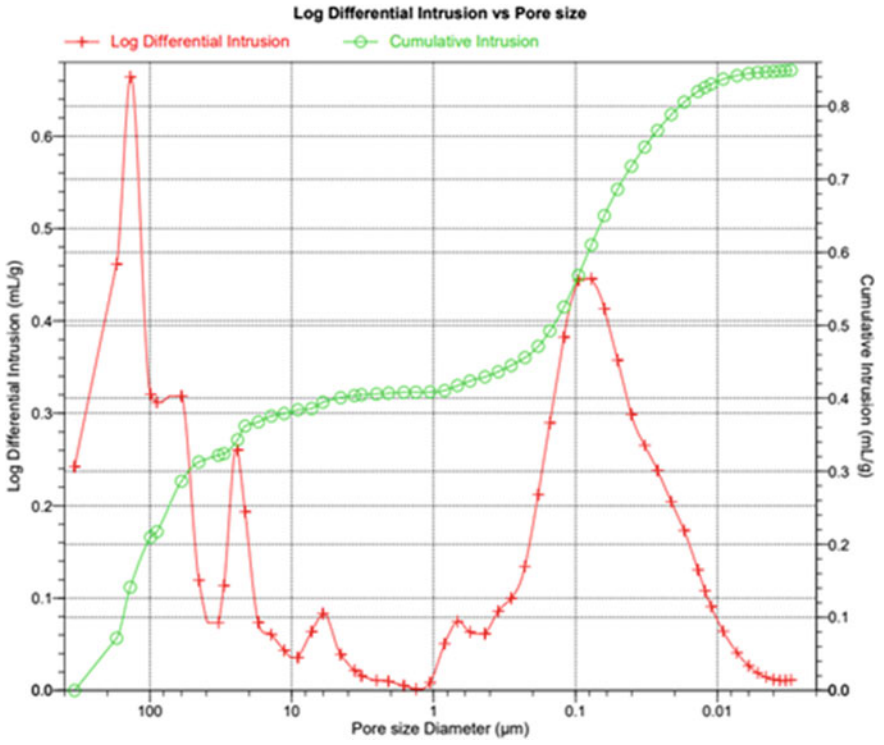

Fig. 13.4 Pore size distribution (reference AAC sample R1)

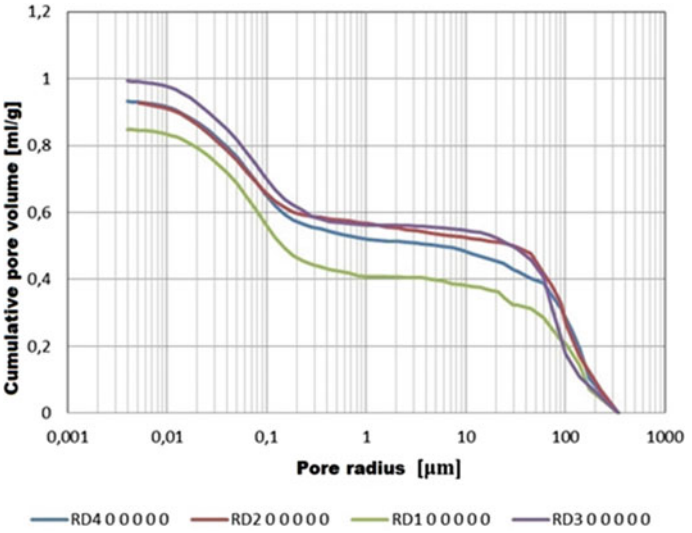

Fig. 13.5 AAC with added high-impact polystyrene (HIPS), distribution of pore geometry in relation to pore sizes

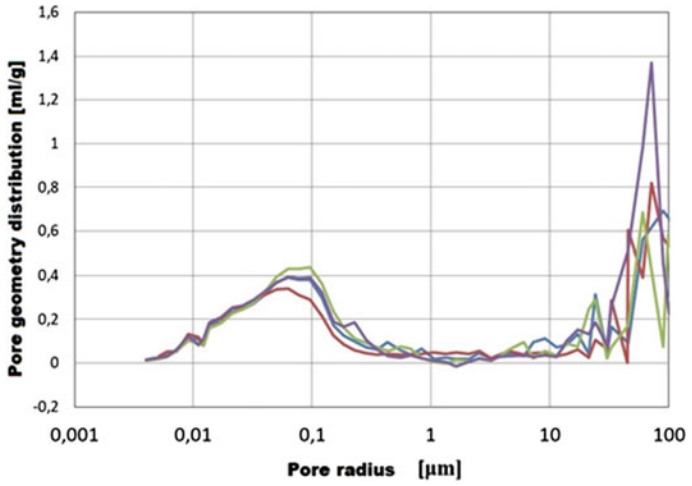

Fig. 13.6 Pore size distribution in AAC with added HIPS

13.4.2 Micro-structure Analysis of AAC Samples

The phase compositions and structure for AAC without and with HIPS was examined utilizing X-ray diffraction (XRD) and Scanning Electron Microscope (SEM) analyses. The area of the specimen was swept by electron probe under voltage of

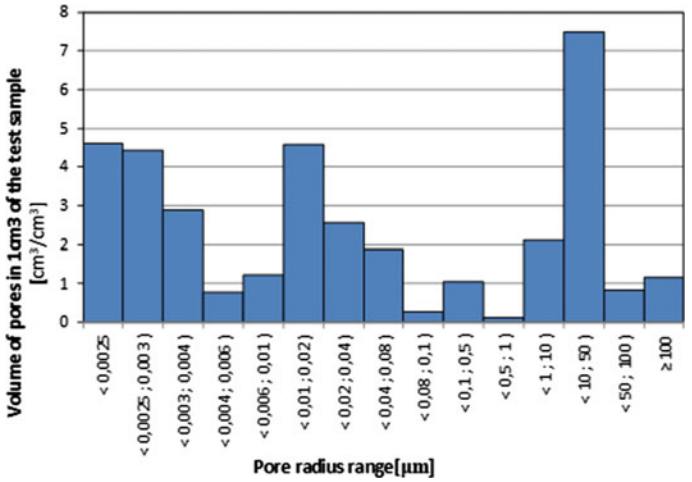

Fig. 13.7 Volume of pores in one m^3 of the test sample as a function of pore sizes

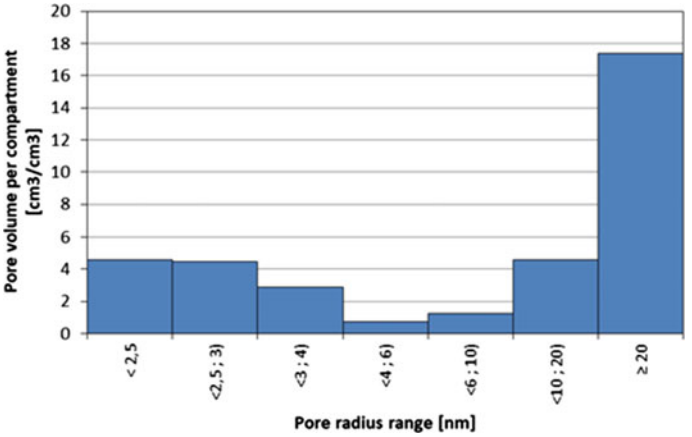

Fig. 13.8 Pore volume in AAC with HIPS in a given compartment as a function of pore radius

5–50 keV. The analysis of the distribution, number, and size of pores is important because this information allows the determination of the relationship between other physico-mechanical and structural values, as well as the durability of the material. Micro CT analysis was performed with the use of the Nikon XT H 225 ST CT scanner, which enabled measurements of external and internal geometry of AAC without and with HIPS (as presented in Fig. 13.9).

Results from measurements of the air void content for four aerated concrete specimens (R1, R2, R3, R4) versus density of the materials analyzed (Table 13.7).

Table 13.7 shows that the addition of HIPS did not significantly affect the number of voids in the modified material, so it certainly did not deteriorate its properties.

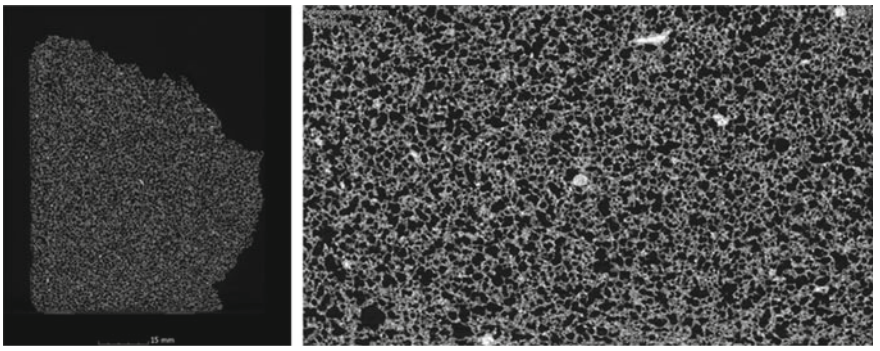

Fig. 13.9 Measurements of pore geometry in the aerated concrete specimens using CT scan technique (computer tomograph)—analysis of distribution, volume, and size of pores in tested material

Table 13.7 Summary of density and air void content in AAC with HIPS

Sample	Bulk density (kg/dm^3)	Air void content (%)
R1	2.3589	52.53
R2	1.9222	47.33
R3	2.3241	55.06
R4	2.2654	55.16
Average value	2.21	52.52

Hydrated calcium silicates (including C-S-H, Tobermorite) are formed in the pores, i.e. phases whose quantity and quality also testify to the effectiveness and durability of the material. These tests showed the presence of pores with sizes of 0.1–100 μm, and the volume of voids in the material was estimated at approximately 50% (RD1 52.53%; RD2 47.33%; RD3 55.06%; RD4 55.16%).

The phase compositions and structure for AAC without and with HIPS was examined utilizing X-ray diffraction (XRD) and Scanning Electron Microscope (SEM) analyses—see Fig. 13.10. The area of the specimen was swept by electron probe under a voltage of 5–50 keV. The analysis of the distribution, number and size of pores is important because this information allows to determine the relationship between other physico-mechanical and structural values, as well as the durability of the material.

The information on the C-S-H phase is particularly important due to the fact that there is an amorphous phase that is formed at the aggregate-binder interface and a metastable phase that strongly reacts to environmental changes (pressure, temperature, or even CO_2 concentration in the atmosphere), which is depends on the concrete pH. Any variations in pH (as a result of external or internal factors) are automatically reflected by the pore count, their sizes, which yields subsequent changes in the structural/physical characteristics of the material.

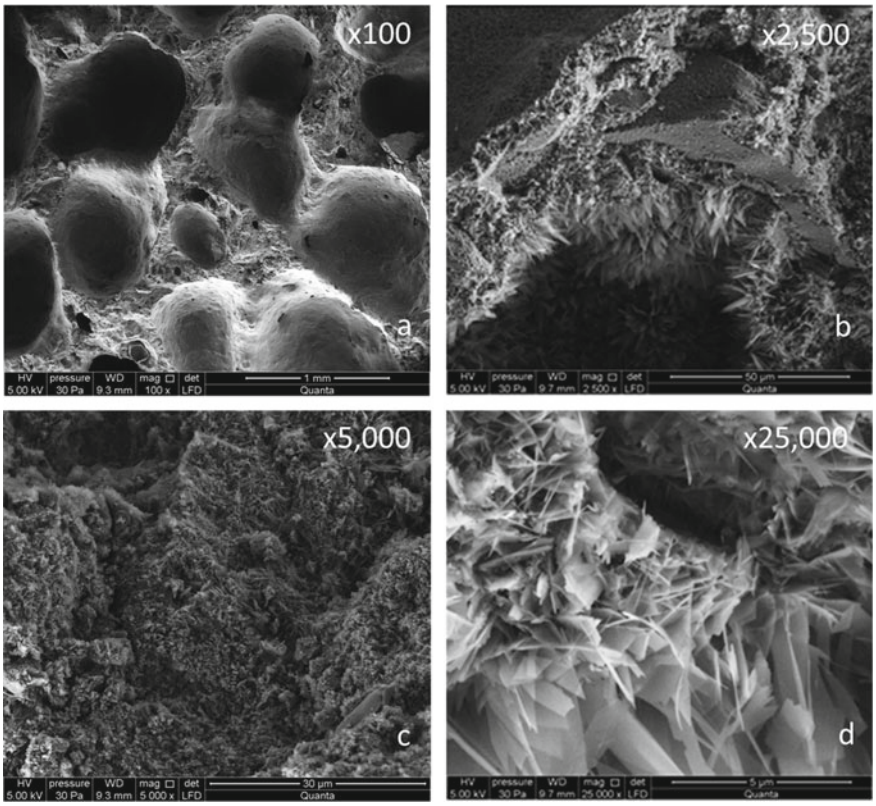

Fig. 13.10 SEM images of the microstructure of ACC with added HIPS: **a** visible pores—100 × magnification, **b** 2,500 × magnification, **c** 5,000 × magnification, and **d** visible Tobermorite—25,000 × magnification

The C-S-H phase has a positive effect on the ACC strength. The following four morphological types of the C-S-H phase exist: (i) fibrous particles of C-S-H, (ii) honeycombs of C-S-H, (iii) flattened/isometric particles of C-S-H, and (iv) spherical agglomerates of C-S-H. Tobermorite has three phases varying by interlayer distances of 1.4; 1.13; and 0.97 nm. (A1 + Na)-substituted Tobermorite structure contain well-developed hexagonal plates that may occur in spherical agglomerations—see: Brelak and Dachowski (2017b), Zapotoczna-Sytek and Balkovic (2013). The SEM analysis of the microstructures of specimens produced from modified AAC revealed the presence of the C-S-H phase and Tobermorite—Richardson (2004). Table 13.8 summarizes the results from the SEM microstructure analysis of AAC. The solid material skeleton, as well as microchannels and pores that constitute the microstructure of AAC materials are shown in Fig. 13.10. The phases that form the solid AAC structure are hydrated calcium silicates with varying degrees of order. The C-S-H phase is an amorphous phase with a sponge-like structure and fills the free spaces in the material.

Table 13.8 Elemental quantitative analysis of sample R1 (AAC with HIPS)

Element	Wt.%	At.%	K-ratio	Z	A	F
C K	1.48	3.35	0.0035	1.0466	0.1793	1.0007
0 K	44.42	60.68	0.0908	1.0289	0.1986	1.0003
Mg K	0.69	0.62	0.0037	0.9871	0.5481	1.0067
Al K	2.50	2.03	0.0166	0.9580	0.6857	1.0119
Si K	24.72	19.24	0.1901	0.9859	0.7770	1.0036
K K	0.59	0.33	0.0053	0.9359	0.9218	1.0448
Ca K	25.24	13.73	0.2311	0.9579	0.9556	1.0000
Total	100.00	100.00	–	–	–	–

Figure 13.11 shows the results of the SEM microstructure assessment with simultaneous elemental composition analysis (EDS spectrum for three randomly picked points on the AAC sample. It can be observed that all three analyzed points show very similar EDS spectra, which indicates high uniformity of tested AAC material. Please also notice that the existence of metallic elements such as aluminum, iron, and magnesium (Table 13.8 and Fig. 13.11) results from a use of industrial sand in the preparation of laboratory specimens of aerated concrete.

In concrete, the first phase to precipitate by chemical reaction is allite, which is responsible for the early strength of the concrete. Alite is calcium oxysilicate, the most important phase in Portland clinker. The reactivity of allite with water is responsible for the hardening of the slurry. Alite is more reactive than belite, due to its higher Ca content and the presence of oxide ions in the crystal lattice. Belite

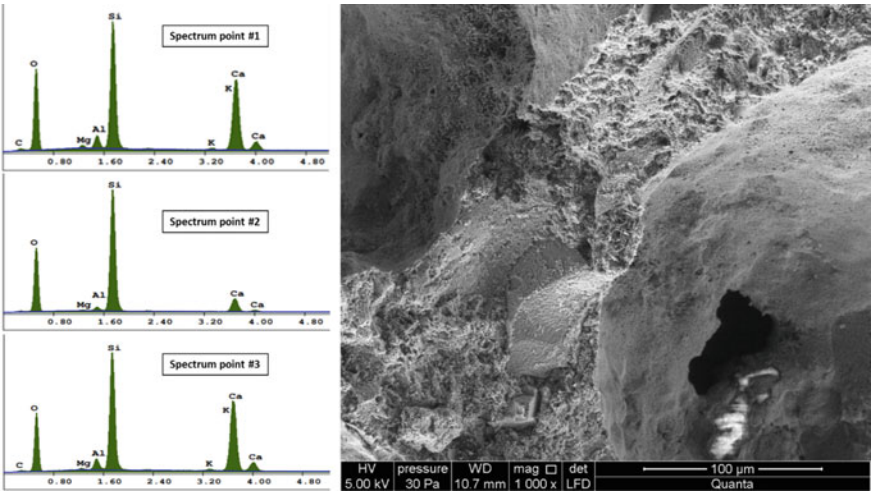

Fig. 13.11 Energy Dispersive X-ray Spectroscopy (EDS) spectrum analysis for three randomly selected points on the AAC sample and SEM view of its microstructure at 1,000 × magnification

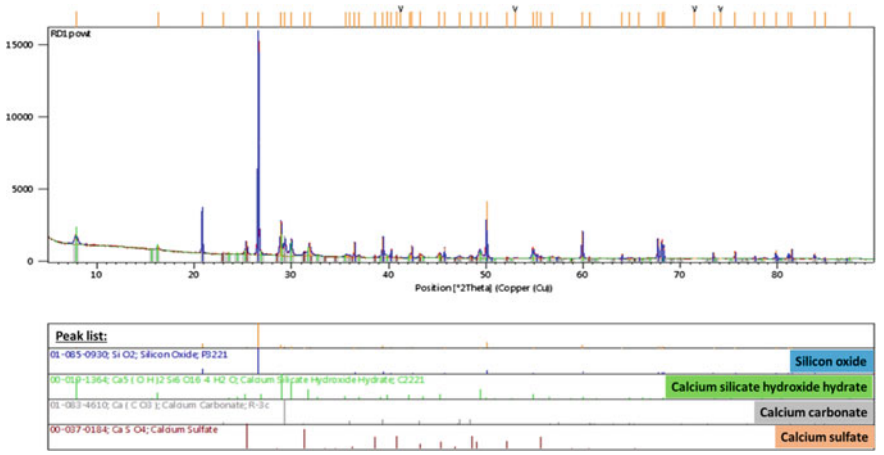

Fig. 13.12 XRD analysis of AAC specimens with HIPS

is a calcium orthosilicate and the second most important mineral component (after allite) in Portland clinker. Belite provides "late" concrete strength due to its lower reactivity—see: Taylor (1997), Matschei et al. (2007).

$$Ca_3[SiO_4]O \;=\; Ca_2[SiO_4] \;+\; CaO$$

$$CaO \;+\; H_2O \;\Rightarrow\; Ca(OH)_2$$

X-Ray Diffraction, frequently abbreviated as XRD, is a non-destructive test method comonly used to analyze the internal structure of crystalline materials. XRD analysis (Fig. 13.12), by way of the study of the crystal structure, is used to identify the crystalline phases present in a material and thereby reveal chemical composition information. Identification of phases is achieved by comparison of the acquired data to that in reference databases. X-ray diffraction is useful for evaluating minerals, polymers, corrosion products, and unknown materials. In most cases, the specimens are analyzed by powder diffraction using specimens prepared as finely ground powders.[22] The quartz peak, in particular, is visible in Fig. 13.11. Typically XRD is performed from 20 θ (theta), however some phases (including Tobermorite and C-S-H) are visible in the lower range of 10–20 θ. In that light, for autoclaved concrete materials, the specifications for the XRD testing may need to be changed in the future.

[22] https://www.element.com/materials-testing-services/x-ray-diffraction#:~:text=X%2DRay%20Diffraction%2C%20frequently%20abbreviated,thereby%20reveal%20chemical%20composition%20information.

Alite is a thermodynamically unstable mineral at temperatures below 1250 °C. But can be maintained in a metastable state at room temperature. Thermodynamically stable minerals do not have the ability to transform or change from one phase to another under optimal conditions. The C-S-H phase is particularly desirable in concretes, it usually contains a disordered and amorphous structure. C-S-H has a large specific surface area and is a thermodynamically stable phase at ambient temperature (20 °C). Toberomite (C-S-H (I) (Tobermorite) & C-S-H (II) (jennite)—are hydrated calcium silicates, with a crystalline structure (formed by the action of high temperature and/or pressure on the C-S-H phase. These phases are characterized by a low specific surface area—see: Dachowski and Kapała (2016), Balonis (2019). Phase transformations are related to so-called, hardening of the binder, i.e. the formation of a crystalline structure. C-S-H phase is responsible for 70–80% of the concrete strength. It is an amorphous phase that crystallizes over the years (concretes from the time of the Roman Empire still crystallize today).[23] When the C-S-H phase crystallizes, its specific surface area changes (decreases) creating free spaces in the pores, which allows e.g. water to interfere with the structure of the concrete and which consequently leads to the destruction of the concrete structure. C-S-H depending on the concentration of $Ca(OH)_2$ ions in the structure of concrete "takes" or "gives up" Ca++ ions, which is related to the appropriate alkalinity of concrete (preferably above 12.4pH),[24,25]—see also: Stepien et al. (2019), Lothenbach et al. (2019), Taylor (1997), Matschei et al. (2007), Balonis (2019).

13.5 Discussion and Conclusions

AAC products are thermally insulating structural materials that have been highly appreciated by construction industries, especially because of widespread applications in single-family housing. AACs are well-known because of their unique thermal insulation and environmental impact characteristics. They have become highly desired consumer products, which is reflected by numerous national building and energy standards, as well as sustainable construction specifications worldwide.

Autoclaved cellular concrete products exhibit compressive strengths up to 6 MPa. Our recent work demonstrated that use of high impact polystyrene (HIPS) additives can help with improvement of physical and mechanical properties (mainly stabilization of the compressive strength) and can cause significant reduction of the water absorption coefficient. The addition of HIPS to ACC acts in a similar way as the addition of fillers to the raw concrete mass. Performed internal structure analysis of AAC

[23] https://www.wprost.pl/nauka/10063718/Cement-z-czasow-Imperium-Rzymskiego-pomoze-stworzyc-super-beton-Naukowcy-odkrywaja-karty.html.

[24] http://budmax.eu/solbet-blmoczki-z-betonu-komorkowego/.

[25] https://www.polskicement.pl/aktualnosci/cembureau-roadmap-2020-2050-ograniczenie-emisji-co2-o-ok-40-na-koniec-dekady.

showed the presence of amorphous phases of the disordered structure C-S-H. Furthermore, micro-CT analysis demonstrated that the average content of air voids in tested AAC samples was around 52% with an average density from four measurements of 2.21 (kg/dm^3). In addition to the component formulation, the internal structure characteristics were also affected by the employed AAC production method.

Performed porosity analysis of used materials (reference samples and modified with HIPS) made it possible to visualize the internal structure of the HIPS-modified AAC, especially the connections and distribution of micro-pores. This was important for better understanding the porosity test results. The analysis of mechanical strength characteristics was complemented with microstructure examination using a scanning electron microscope (SEM) and XRD, which in turn allowed the observation of hydrated calcium silicates formed in the tested materials. Research data discussed in this chapter demonstrated that the addition of HIPS did not change the microstructure of the material. Considering that cellular concretes are usually designed for a minimum of 20 years of use to further validate the long-term performance of AAC with added of HIPS thermal stability of concrete additives and durability of AAC under variable environmental conditions needs to be investigated.

Acknowledgements The authors would like to acknowledge to: Szmidt A. and Stepien K. for the opportunity to conduct joined analyses on the production of autoclaved materials; Sitarz M., Leśniak M. from AGH University in Cracow, Poland, as well as Skowera K. and Durlej M. from University of Technology in Kielce for cooperation and support.

Funds The Mirco CT analysis tomograph (CENWIS, University of Technology in Kielce), and some of the research done was performed thanks to the endowment funding.

References

Abdulrahman, A., & Bruce N. E. (2004). Super HIPS: Improved high IM pact polystyrene with two sources of rubber particles. *Polymer, 45*, 8435–8442.

Alfarraj, A., & Nauman, E. B. (2004). Super HIPS: Improved high impact polystyrene with two sources of rubber particles. *Polymer, 45*, 8435–8442.

Balonis, M. (2019). Thermodynamic modelling of temperature effects on the mineralogy of Portland cement systems containing chloride. *Cement and Concrete Research, 120*, 66–76. https://doi.org/10.1016/j.cemconres.2019.03.011.

Birkenmajer, K. (1967). Lower Silesian basalts as monuments of inanimate nature—Nature protection No 32. Bazalty dolnośląskie jako zabytki przyrody nieożywionej. Ochrona Przyrody (nr 32, pp. 225–276). Kraków.

Błaszczyński, T. Z., & Król, M. (2013). Geopolimery w budownictwie/Geopolymers in construction. *IZOLACJE,* (5), 38–44.

Błaszczyński, T. Z., & Król M. (2014). Concrete production and the problem of reducing carbon dioxide emissions. *IZOLACJE*, (3). https://www.izolacje.com.pl/artykul/chemia-budowlana/166160,produkcja-betonu-a-problem-redukcji-emisji-dwutlenku-wegla. Accessed 01 July 2021.

Boltyanskii, A. V., Bulakh, V. L., & Fedorova, L. S. (1995). Use of industrial waste for the production of building materials. *Refractories and Industrial Ceramics, 36*(8).

Brelak, S., & Dachowski, R. (2017a). Multi-criteria comparative analysis of products made of autoclaved aerated concrete modified with recycling materials. Wielokryterialna analiza porównawcza wyrobów z autoklawizowanego betonu komórkowego modyfikowanego materiałami recyklingowymi. Budownictwo o Zoptymalizowanym Potencjale Energetycznym, *2*(20), 29–36. https://doi.org/10.17512/bozpe.2017a.2.04.

Brelak, S., & Dachowski, R. (2017b). Effect of autoclaved aerated concrete modification with high-impact polystyrene on sound insulation. *IOP Conference Series: Materials Science and Engineering, 245.*

Dachowski, R., & Kapała, S. (2016). Modification of autoclaved aerated concrete with high-impact polystyrene. Materiały Budowlane, Wydawnictwo SIGMA-NOT Sp. z o.o., Redakcja Materiały Budowlane (Vol. 6, pp. 69–70), Warsaw.

EU PN (2004) Directive 2002/91/EC of 16 December 2002 on the energy performance of buildings. Standard PN-EN ISO 13790, Standard PN-EN ISO 6946. https://www.iea.org/policies/712-energy-performance-of-buildings-directive-200291ec.

Gawin, D., & Kośny, J. (2000). Effect of moisture on thermal performance and energy efficiency of buildings with lightweight concrete walls. In *Proceedings of the 2000 ACEEE Conference, ACEEE Summer Study on Energy Efficiency in Buildings: American Council for an Energy Efficient Economy*, Pacific Grove.

Gawin, D., Kośny, J., & Wilkes, K. E. (2004). Thermal conductivity of moist cellular concrete—Experimental and numerical study. In *IX Conference—Thermal Performance of the Exterior Envelopes of Buildings*, Clearwater, Florida.

Kapała, S., & Dachowski, R. (2016). The influence of the chalcedony on the properties of autoclaved aerated concreto. *Procedia Engineering,* 699–703.

Kejkar Rupali, B., & Wanjari Swapnil, P. (2021). Feasibility study of commercially viable sustainable aerated geopolymeric foam based block. *Materials Today, 45*, 4398–4404 (Elsevier). https://doi.org/10.1016/j.matpr.2020.11.916.

Kozłowski, S. (1975). Rock raw materials of Poland/Surowce skalne Polski-Wydawnictwo geologiczne/Geological Publishing House.

Li, F., Chen, G., Zhang, Y., Hao, Y., & Si, Z. (2020). Fundamental properties and thermal transferability of masonry built by autoclaved aerated concrete self-insulation blocks. *Materials (Basel), 13*(7), 1680. https://doi.org/10.3390/ma13071680.

Lothenbach, B., Kulik, D. A., Matschei, T., Balonis, M., Baquerizo, L., Dilnes, B., Miron, J. D., & Myers, R. J. (2019). Cemdata18: A chemical thermodynamic database for hydrated Portland cements and alkali-activated materials. *Cement and Concrete Research.*

Macech, J. (2020). Fire resistance of construction products. Association of silicate producers. White Bricklaying. https://budownictwob2b.pl/przegrody/baza-wiedzy/sciany-i-stropy/22854-odpornosc-ogniowa-wyrobow-budowlanych.

Matschei, T., Lothenbach, B., Glasser, F. P. (2007). The role of calcium carbonate in cement hydration. *Cement and Concrete Research.*

Nonat, A., Lecoq, X. (1998). The structure, stoichiometry and properties of C-S-H prepared by C3S hydration under controlled condition. In *Nuclear magnetic resonance spectroscopy of cement-based materials* (pp. 197–207). Springer, Berlin, Heidelberg. https://doi.org/10.1007/978-3-642-80432-8_14.

Parker, P. M., Lilly, E. (2005). The 2006–2011 World Outlook for All Silica. Brick and shapes excluding Semi-Silica. INSEAD (Singapore and Fontainebleau, France) ICON Group International, Inc.

Polyzois, D., & Raftoyiannis Ioannis, G. (2007). The effect of semi-rigid connections on the dynamic behavior of tapered composite GFRP poles. *Composite Structures, 81*(1), 70–79.

Pruteanu, M., & Vasilache, M. (2013). Thermal conductivity determination for autoclaved aerated concrete elements used in enclosure masonry walls. *Bulletin of the Polytechnic Institute of Jassy, CONSTRUCTIONS. ARCHITECTURE Section, LIX*(LXIII)(3), 33–42.

Richardson, I. (2004). Tobermorite/jennite- and tobermorite/calcium hydroxide-based models for the structure of C-S-H: Applicability to hardened pastes of tricalcium silicate, beta-dicalcium

silicate, Portland cement, and blends of Portland cement with blast-fumace slag, metakaolin, or silica fume. *Cement and Concrete Research, 34*, 1733–1777.

Rybarczyk, T., Chojnowski, J., Chruściel, W., Janiak, R., Kwaśniak, J., & Łaskawiec, K. (2015) Almost everything about cellular concrete/Prawie wszystko o betonie komórkowym. Zeszyt 1, Stowarzyszenie Producentów Betonów, Warszawa. ISBN 978-83-941005-1-3. http://s-p-b.pl/img/upload/Prawie%20wszystko%20o%20betonie%20kom%C3%B3rkowym0.pdf.

Skalmowski, W. (1966). Technology of building materials/Technologia materiałów budowlanych Arkady, Tom II, Warszawa.

Stepien, A., Leśniak, M., & Sitarz, M. (2019). A sustainable autoclaved material made of glass sand. *MDPI, Buildings, 9*(11), 232.

Stepien, A., Potrzeszcz-Sut, B., Balonis, M., Prentice, D. P., Oey, T. (2020) The role of glass compounds in autoclaved bricks. *Buildings (MDPI),* Tom: 10, Zeszyt: 3, Strony: 1–25.

Szoke, S. S. (2014) Guide to thermal properties of concrete and masonry systems. American Concrete Institute, ACI 122R-14, ISBN: 978-0-87031-971-6.

Taylor, H. F. W. (1997). *Cement chemistry* (p. 459). Thomas Telford. ISBN: 0 7277 2592 0.

Van Boggelen, W. (2014). History of autoclaved aerated concrete—The short story of a long lasting building material.

Vilaplana, F., Ribes-Greus, A., & Karlsson, S. (2010). Chromatographic pattern in recycled high-impact polystyrene (HIPS)—Occurrence of low molecular weight compounds during the life cycle. *Polymer Degradation and Stability, 95*, 172–186.

Wcisło, A. (2018). Green construction of gray concreto/Zielone budownictwo z szarego betonu. Lafarge Cement S.A., DNI BETONU.

Zapotoczna-Sytek, G., & Balkovic, S. (2013). Autoclaved aerated concrete. Technology, properties, application/Autoklawizowany beton komórkowy. Technologia, właściwości, zastosowanie-Wydawnictwo Naukowe PWN, Warszawa.

Zapotoczna-Sytek, G. (2018). Durability of autoclaved aerated concrete based on Polish experience. In *ICAAC—6th International Conference on Autoclaved Aerated Concrete* (Vol. 2, No. 4, pp. 53–62). https://doi.org/10.1002/cepa.850.